The PIP2 binding mode of the C2 domains of rabphilin-3A

PIERRE MONTAVILLE,[1,3] NICOLAS COUDEVYLLE,[1,3] ANAND RADHAKRISHNAN,[2] ANDREI LEONOV,[1] MARKUS ZWECKSTETTER,[1] AND STEFAN BECKER[1]

[1]Department of NMR-based Structural Biology, Max-Planck-Institute for Biophysical Chemistry, 37077 Göttingen, Germany
[2]Department of Neurobiology, Max-Planck-Institute for Biophysical Chemistry, 37077 Göttingen, Germany

Abstract

Phosphatidylinositol-4,5-bisphosphate (PIP2) is a key player in the neurotransmitter release process. Rabphilin-3A is a neuronal C2 domain tandem containing protein that is involved in this process. Both its C2 domains (C2A and C2B) are able to bind PIP2. The investigation of the interactions of the two C2 domains with the PIP2 headgroup IP3 (inositol-1,4,5-trisphosphate) by NMR showed that a well-defined binding site can be described on the concave surface of each domain. The binding modes of the two domains are different. The binding of IP3 to the C2A domain is strongly enhanced by Ca^{2+} and is characterized by a K_D of 55 μM in the presence of a saturating concentration of Ca^{2+} (5 mM). Reciprocally, the binding of IP3 increases the apparent Ca^{2+}-binding affinity of the C2A domain in agreement with a Target-Activated Messenger Affinity (TAMA) mechanism. The C2B domain binds IP3 in a Ca^{2+}-independent fashion with low affinity. These different PIP2 headgroup recognition modes suggest that PIP2 is a target of the C2A domain of rabphilin-3A while this phospholipid is an effector of the C2B domain.

Keywords: C2 domain tandem; rabphilin-3A; IP3; calcium-binding protein; NMR; protein/ligand docking; HADDOCK

Supplemental material: see www.proteinscience.org

Rabphilin-3A is a cytosolic neuronal protein that is involved in the neurotransmitter release cycle. Although not fully clarified yet, its function is related to specific stages of regulated vesicle cycling processes such as the inter-action of vesicles with the actin cytoskeleton (Baldini et al. 2005), the docking of these vesicles to the plasma membrane (Tsuboi and Fukuda 2005), the re-priming of vesicles after extensive evoked neurotransmitter release (Deak et al. 2006), and a so far unidentified step of the endocytosis (Ohya et al. 1998). Rabphilin-3A consists of an N-terminal Rab small GTPase binding domain, a linker region of unknown function, and a C-terminal tandem of C2 domains (C2A and C2B) involved in the Ca^{2+}-dependent membrane targeting of the protein (Fig. 1). These C2 domains are essential for the functions of rabphilin-3A in the synaptic vesicle trafficking process. They have been described to interact with the SNARE protein SNAP25 (Tsuboi and Fukuda 2005), β-adducin (Miyazaki et al. 1994), CASK (Zhang et al. 2001), and annexin A4 (Willshaw et al. 2004). However, the primary targets of these C2 domains are the membrane
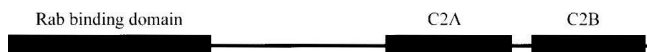
Figure 1. Structural organization of rabphilin-3A. The bar graph depicts the domains of rabphilin-3A whose three-dimensional structures have been solved: the Rab binding domain, the C2A domain, and the C2B domain.

phospholipids phosphatidylserine (PS) and phosphatidylinositol-4,5-bisphosphate (PIP2). The latter represents <1% of the lipids in the plasma membrane and forms microdomains to regulate several signaling events (Golub and Caroni 2005; Osborne et al. 2006). More specifically, PIP2 is involved in different stages of the neurotransmitter release process. It is required for clathrin-mediated endocytosis (Haucke 2005), for specific stages of exocytosis, and synaptic vesicle trafficking (Osborne et al. 2006). PIP2 recruits proteins to specific locations in the plasma membrane to modulate spatially localized events involved in membrane traffic (Cremona and De Camilli 2001). Although not known to be a classical phosphoinositide-binding module, some C2 domains have been described to interact rather specifically with phosphoinositides, especially with PIP2 (Cho and Stahelin 2006). The C2 domain of PKCα is, so far, the best functionally and structurally characterized PIP2-interacting C2 domain. This interaction is essential for the proper subcellular localization of PKCα (Rodríguez-Alfaro et al. 2004; Evans et al. 2006). A set of basic residues located at the concave side of its C2 domain is essential for binding PIP2 (Corbalán-García et al. 2003; Marín-Vicente et al. 2005). Several C2 domains of proteins involved in synaptic vesicle fusion have been described to bind PIP2, e.g., C2 domains of synaptotagmins (Tucker et al. 2003), CAPS-1 (Grishanin et al. 2004), and rabphilin-3A (Chung et al. 1998). The binding of the C2B domain of synaptotagmin 1 to PIP2 prelocalizes the protein to PIP2-enriched membranes (Schiavo et al. 1996) and increases the speed response of synaptotagmin 1 in SNARE complex-mediated liposome fusion (Bai et al. 2004). Recently, a role for the CAPS-1 PIP2 interaction has been shown in the pre-fusion step of dense core vesicle fusion (Grishanin et al. 2004). Contrary to synaptotagmin 1 and 11, which bind PIP2 via their C2B domain only, and synaptotagmin 3 and 7, which bind PIP2 via their C2A domain only (Tucker et al. 2003), both C2 domains of rabphilin-3A have been shown to interact with PIP2. No functional role for this interaction has been attributed so far, although rabphilin-3A is involved in processes regulated by PIP2 (Chung et al. 1998).

PIP2 is a common player between the cytoskeleton-membrane attachment, the vesicle docking, and endocytosis in the neurotransmitter release process. Since rabphilin-3A is involved in these processes, its PIP2 binding properties via its C2 domains might be important to elucidate its function. In this context we undertook to characterize the PIP2 headgroup binding properties of both C2 domains using NMR spectroscopy. In addition to the structural features, relative affinities in solution and the Ca^{2+} dependency of these interactions were addressed. The combination of our NMR data and a C2A/IP3 complex docking model allow the prediction of specific functions for both C2 domains in vesicle trafficking.

Results

Glycerophosphoserine interaction with the C2A and C2B domain of rabphilin-3A

Before addressing PIP2 headgroup recognition by the C2 domains of rabphilin-3A, we investigated if the two domains interact in a specific manner with glycerophosphoserine (GPS), the headgroup of their main phospholipid target PS (Yamaguchi et al. 1993). ^{15}N-^{1}H HSQC-based titrations of GPS to the C2A and the C2B domains in the presence of a saturating Ca^{2+} concentration (5 mM, see below) up to 20 mM GPS did not induce chemical shift perturbation in the Ca^{2+}-binding regions of the two domains. Thus, no specific PS headgroup recognition site can be described in the CBR of these domains, albeit PS is their primary target.

Ca^{2+}- and IP3-binding mode of the C2A domain

The crystal structure of the C2A domain of rabphilin-3A did not contain any ordered Ca^{2+} ions (Biadene et al. 2006). Therefore we probed the Ca^{2+}-binding properties of this C2 domain by NMR. A ^{15}N-^{1}H HSQC-based Ca^{2+} titration from 0 to 20 mM mainly induced chemical shift changes of residues located in the Ca^{2+}-binding region (CBR) (Fig. 2A), in agreement with previous observations concerning the ability of this domain to bind Ca^{2+} (Montaville et al. 2007). The N- and C-terminal extremities are moderately affected as well, which is explained by their spatial proximity to the CBR. Saturation of the C2A domain was reached at 5 mM Ca^{2+}. No additional low affinity Ca^{2+}-binding site was found at higher concentrations. Fitting the chemical shift perturbations of residues located in the neighborhood of the CBR against Ca^{2+} concentration was possible with Equation 3 (see Materials and Methods), indicating cooperative binding. A global dissociation constant of 1.1 ± 0.01 mM with a Hill coefficient of 2.24 ± 0.03 was obtained (Fig. 2B). This indicates that two Ca^{2+} ions bind in a cooperative way to the C2A domain of rabphilin-3A.

D-myo-Inositol-1,4,5-trisphosphate (IP3, i.e., PIP2 headgroup) titration of the C2A domain in a saturating concentration of Ca^{2+} (5 mM) showed large chemical
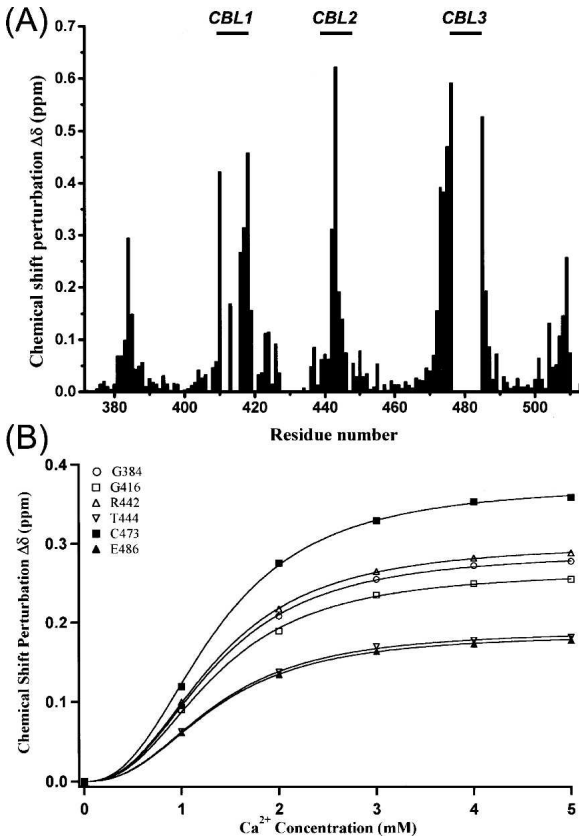
Figure 2. Ca^{2+}-binding properties of the C2A domain of rabphilin-3A. (*A*) ^{1}H-^{15}N chemical shift perturbations δΔ (see Materials and Methods) plotted against the sequence of the C2A domain fragment (371–510) upon addition of 5 mM Ca^{2+}. Missing chemical shift deviations are associated with cross-peaks in intermediate chemical exchange rates at pH 7.0 in the absence of Ca^{2+} and with proline residues. The positions of the three Ca^{2+}-binding loops (CBL1, CBL2, and CBL3) are highlighted on *top*. (*B*) Simultaneous fit performed on the chemical shift perturbations of six residue backbone HN cross-peaks according to the Ca^{2+} concentration using the Hill equation (Equation 3; see Materials and Methods).

shift perturbations for a limited set of residues located on the concave side of the core domain (site1) (Fig. 3A). The binding occurs on the fast exchange timescale, indicating a rather low affinity for the ligand in solution, although the recognition for IP3 involves a well-defined binding site. In addition, HN resonances belonging to residues from CBL3 and the loop between the β3 and β4 strands were broadened out at pH 7.0 but appeared in the spectra for high IP3 concentrations (data not shown). This indicates that the overall dynamics of these two loops surrounding the β-groove of the C2A domain change upon the binding and that these loops are probably actively involved in the binding. The saturation was reached with a fivefold excess of the ligand. A simultaneous fit

with Equation 1 (see Materials and Methods) using chemical shift perturbations from 12 HN cross-peaks gave a K_D value of 55 ± 4 μM (Fig. 3B).

A second subset of HN cross-peaks from residues located mainly on CBL2 and CBL1 (site 2) (Fig. 3A) was affected differently by IP3-binding compared to residues located on the concave side of the core domain (site 1). Indeed, the IP3-binding for residues N443 and T444 on CBL2 and G416, L417 on CBL1 (Fig. 3C) is described by sigmoidal curves. The IP3 concentration corresponding to 50% binding is higher compared to the binding curves of residues from site 1. A simultaneous fit of chemical shift perturbations from cross-peaks of residues G416, L417 (CBL1), N443, and T444 (CBL2) using Equation 2 (see Materials and Methods), which takes into account the free ligand concentration depleted by the binding to the first site, gave a K_D of 540 ± 45 μM (Fig. 3C). These observations indicate a second low affinity IP3-binding site (defined as site 2), involving residues located on CBL2 and CBL1 (Fig. 3A). Because both sites are topologically close to each other, cooperativity might occur in IP3-binding. To probe this, the binding curves corresponding to the residues of site 1 were fitted with Equation 3. The fitted data were identical to those obtained using Equation 1 with a Hill coefficient of 0.95 ± 0.02, indicating no cooperativity between both sites.

Ca^{2+} dependency of IP3-binding to the C2A domain

To investigate possible cooperativity between Ca^{2+} and IP3-binding we performed an IP3 titration of the C2A domain without adding Ca^{2+} to the buffer. The saturation was reached at about 10 mM IP3 (Fig. 4A). A simultaneous fit of the affected residues with Equation 1 worked for all residues except for K423, L427, and L468, which may experience secondary effects in the presence of very high IP3 concentrations (Fig. 3A). Fitting the other affected residues resulted in a K_D of 800 ± 50 μM, indicating that in the absence of Ca^{2+} the affinity of the C2A domain is about 16 times lower than in the presence of saturating concentrations of Ca^{2+}. This shows that Ca^{2+} promotes IP3-binding. Next, we performed a Ca^{2+} titration in the presence of saturating (10 mM) IP3 (Fig. 4B). The simultaneous fit of the affected residues using Equation 3 (see Materials and Methods) resulted in a K_D of 320 ± 9 μM with a Hill coefficient of 1.49 ± 0.04, indicating a limited decrease in the cooperativity of Ca^{2+}-binding in the presence of saturating IP3. The Ca^{2+} affinity is increased threefold under these conditions. These data show that IP3, despite its low intrinsic affinity, is able to promote the recruitment of Ca^{2+}, revealing cooperativity between Ca^{2+} and IP3-binding to the C2A domain of rabphilin-3A.
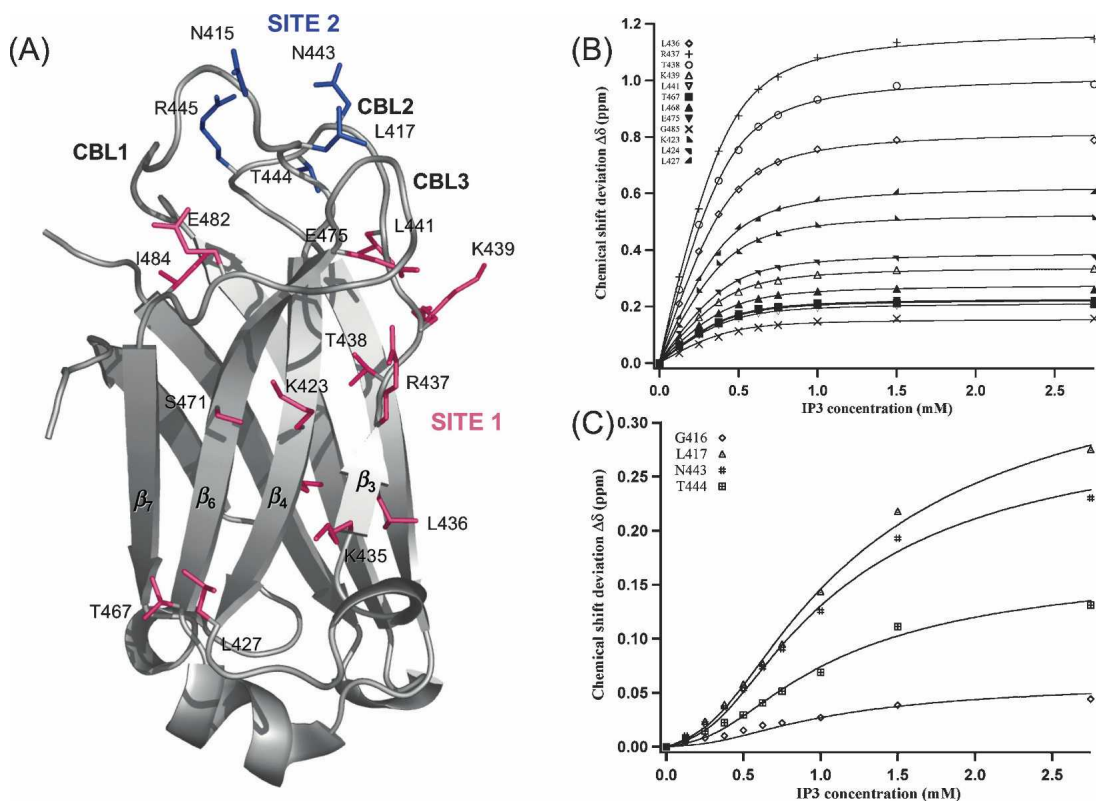
Figure 3. IP3-binding mode of the C2A domain of rabphilin-3A. (*A*) Residues whose ^{1}H-^{15}N cross-peaks experienced significant chemical shift perturbations in the presence of 2.75 mM IP3 and 5 mM Ca^{2+} are mapped on the C2A domain crystal structure (PDB access number 2chd). Residues defining site 1 are colored in magenta; residues defining site 2 are colored in blue. (*B*) Simultaneous fit performed on chemical shift perturbation of 12 residue backbone HN cross-peaks from IP3-binding site 1 upon IP3 titration in the presence of 5 mM Ca^{2+} using Equation 1 (see Materials and Methods). (*C*) Simultaneous fit performed on chemical shift perturbation of four residue backbone HN cross-peaks upon IP3 titration in the presence of 5 mM Ca^{2+} using Equation 2 (see Materials and Methods). These residues correspond to the second IP3-binding site (site 2).

IP3-binding to the C2B domain

Next, IP3 was used to probe how the C2B domain of rabphilin-3A may bind the PIP2 headgroup. In the presence of 1 mM Ca^{2+}, a ^{15}N-^{1}H HSQC-based IP3 titration showed chemical shift perturbations of a restricted number of cross-peaks in the C2B domain spectrum (Fig. 5A), contrary to PS (Montaville et al. 2007). Similar to the C2A domain, all affected residues are located in the concave basic groove of the C2B domain. However, IP3-binding does not only affect residues of β-strands 3 and 4, but also of β-strands 6 and 7 (Fig. 5B). Unexpectedly, the strongest shifts are observed for polar residues located at the C-terminal tail of rabphilin-3A, namely His 680, Ser 682, and Ser 683. This C-terminal tail (Q674–D684) is considered to be flexible, as most of it was not included in the NMR structure of the C2B domain (Ubach et al. 1999) nor were these residues ordered in the crystal structures (Montaville et al. 2007) of this domain. Noteworthy, E678 is located in both structures in the vicinity of β-

strand 7, orienting the last flexible residues toward the concave side of the C2B domain (Supplemental Fig. 1). Thus the chemical shift perturbations observed for the residues located on β-strand 7 may be an indirect effect from the strongly affected C-terminal tail residues upon IP3-binding. The interaction of IP3 with the core domain residues takes place in the fast exchange rate timescale, indicating a rather low affinity, which was expected in the absence of the membrane interface. For these residues the chemical shift deviations plotted against the total IP3 concentration could be fitted with a single binding-site model (Equation 1; Fig. 5C). A dissociation constant of 0.54 ± 0.03 mM was obtained by fitting simultaneously the chemical shift perturbations of 11 residues (see Fig. 5C) involved directly or indirectly in IP3-binding.

The overlay of the IP3-bound C2B domain spectra in the presence and absence of Ca^{2+} showed that cross-peaks of the residues that are involved in IP3-binding stay IP3 bound even in the absence of Ca^{2+} (Fig. 6), indicating that
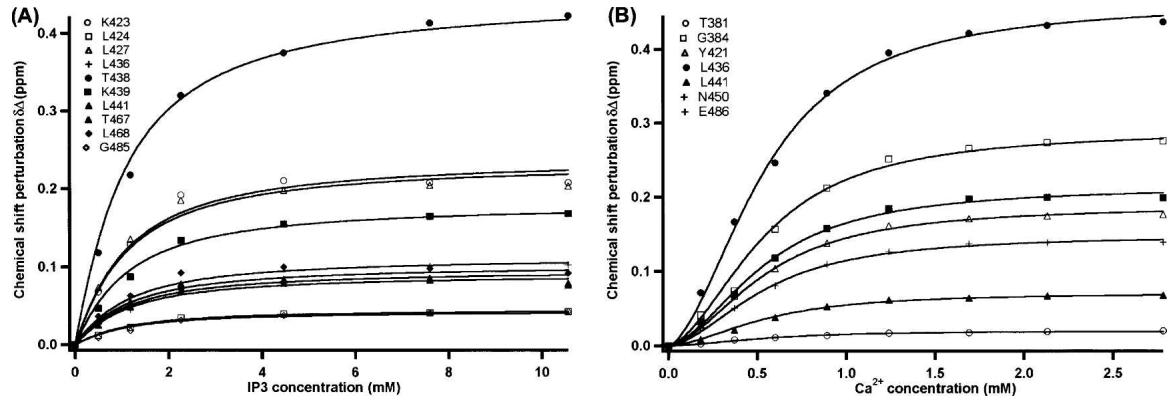
Figure 4. Ca^{2+} dependency of IP3-binding to the C2A domain. (*A*) Simultaneous fit performed on chemical shift perturbation of 10 residue backbone HN cross-peaks from IP3-binding site 1 upon IP3 titration without addition of Ca^{2+} to the buffer using Equation 1 (see Materials and Methods). (*B*) Simultaneous fit performed on the chemical shift perturbations of seven residue backbone HN cross-peaks according to the Ca^{2+} concentration using the Hill equation (Equation 3; see Materials and Methods) in the presence of 10 mM IP3.

IP3-binding does not depend on Ca^{2+}-binding. To validate the use of IP3 to probe the PIP2 binding site on the C2B domain, we used submicellar concentrations of 1,2-dioctanoyl-PIP2 (DOPIP2). Monomeric DOPIP2 induced HN cross-peak shifts corresponding to chemical shift perturbations for the same set of residues promoted by moderate IP3 concentrations (data not shown).
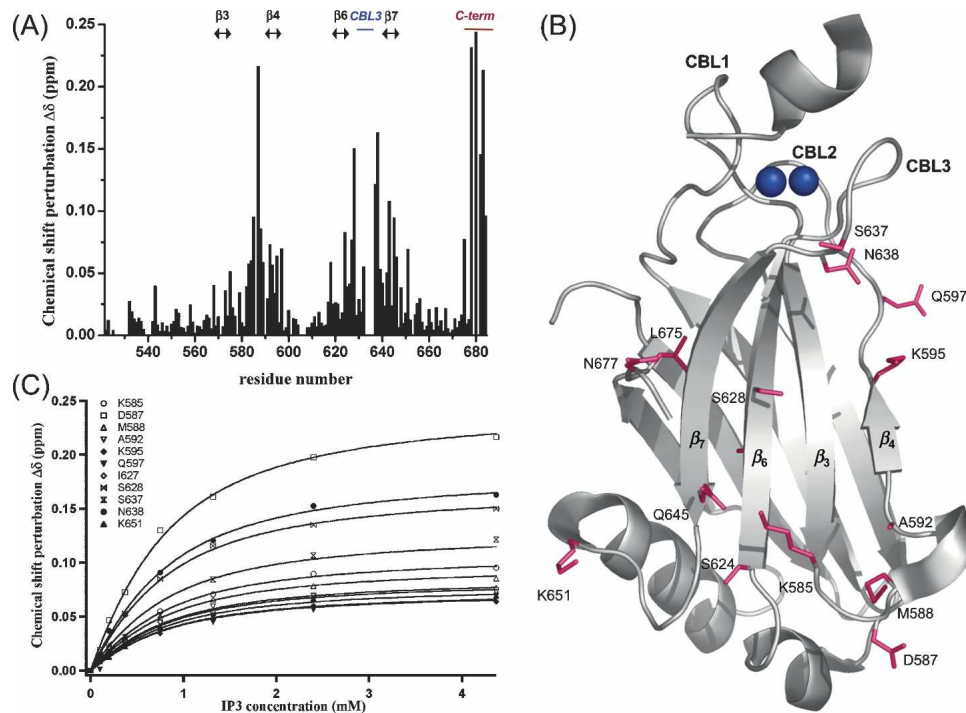

Figure 5. IP3-binding mode of the C2B domain of rabphilin-3A. (*A*) ^{1}H-^{15}N chemical shift perturbations δΔ (see Materials and Methods) plotted against the sequence of the C2B domain fragment (519–684) upon the addition of 4.3 mM IP3 in the presence of 1 mM Ca^{2+}. The secondary structure elements involved in the binding, β-strands 3, 4, 6, and 7, the Ca^{2+}-binding loop 3, and the C-terminal tail are highlighted on *top*. (*B*) Residues experiencing ^{1}H-^{15}N chemical shift perturbations larger than 0.07 ppm upon IP3 titration are mapped on the C2B crystal structure (PDB accession number 2cm6, chain B). (*C*) Simultaneous fit performed on chemical shift perturbations of 11 residue backbone HN cross-peaks according to IP3 concentration using Equation 1 (see Materials and Methods).
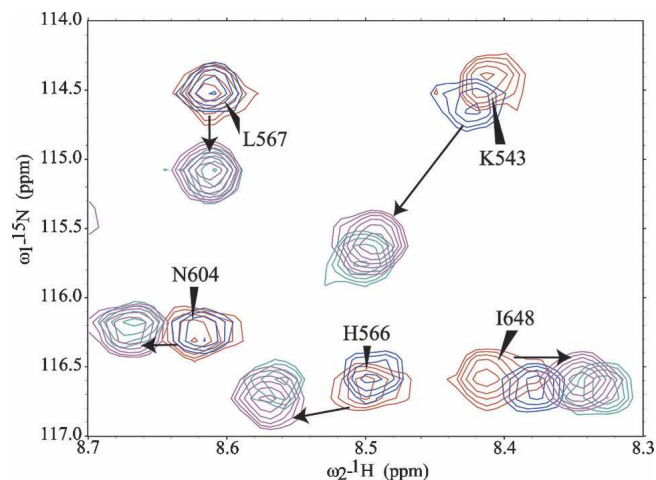
Figure 6. Ca^{2+}-independent IP3-binding to the C2B domain. Overlay of a region of ^1H-^{15}N HSQC C2B domain spectra. Red resonances correspond to the Ca^{2+}-bound C2B domain (1 mM Ca^{2+}), blue resonances to the Ca^{2+} free C2B domain (10 mM EGTA), magenta resonances to the Ca^{2+}- and IP3-bound C2B domain (1 mM Ca^{2+}, 4 mM IP3), and cyan resonances to the Ca^{2+} free, IP3-bound C2B domain (10 mM EGTA, 4 mM IP3). The black arrows indicate the chemical shift deviations of the cross-peaks (Ca^{2+} free and bound) upon IP3-binding.

Docking PIP2 on binding site 1 of the C2A domain

The docking procedure was driven using the crystal structure of the C2A domain (Biadene et al. 2006) as starting coordinates. PIP2 (1,2-diacetoyl-sn-3-[phosphoinositol-3,4,5-trisphosphate]) was docked in order to mimic a polar head from a lipid embedded in the plasma membrane. Ambiguous intermolecular restraints were defined between the protein and the IP3 moiety of PIP2 in order to match the experimental conditions. Statistical data for the final ensemble are summarized in Supplemental Table 2.

Energetic criteria are satisfying, with High Ambiguity Driven protein–protein DOCKing (HADDOCK) scores of -1724 ± 4 kCal.mol^{-1} for the C2A/PIP2 complex. Within the ensemble of the 50 final structures a single cluster was obtained. Hence, ligand position and orientation are well conserved over the ensemble as also shown by the rather low RMSD values measured at the protein/ligand interface: 1.90 ± 0.62 Å.

Examination of the three most representative structures (Fig. 7A) for the C2A/PIP2 complex (site 1) shows that position and orientation of PIP2 are relatively well defined. As shown in Figure 7B, the PIP2 molecule binds to the concave side of the domain via direct interactions between the phosphate moieties 4 and 5 of the PIP2 headgroup and basic residues from β-strands 3 and 4 (Lys_{423}, His_{425}, Lys_{435}, and Arg_{437}). This interaction mode positions the main axis of the phospholipid headgroup perpendicular with respect to the plane defined by the β-sheet. This docking model resembles the model for PIP2 binding of the C2 domain of PKCα (Sanchez-Bautista et al. 2006).

Discussion

The C2A domain as a PIP2 targeting module

Rabphilin-3A is, so far, the only known C2 domain tandem containing protein where both C2 domains bind PIP2 (Chung et al. 1998). This phospholipid is known to play an essential role in the trafficking of neurotransmitter-enriched vesicles. Functional roles of the C2B domain have been postulated for this process, whereas the function of the C2A domain remains elusive. Here, we have shown that the binding modes of both C2 domains of rabphilin-3A to the PIP2 headgroup differ in affinity as well as in Ca^{2+} dependency.
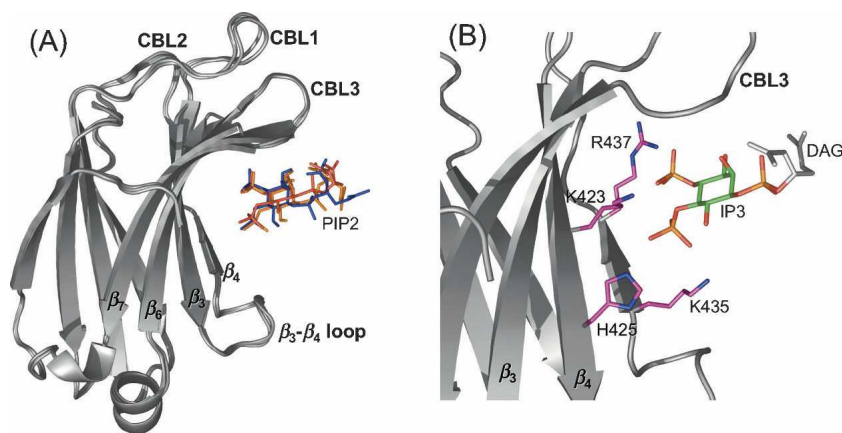
Figure 7. Docking model for the C2A/PIP2 complex. (*A*) Ribbon representation of the final ensemble of models for the C2A/PIP2 complex. PIP2 is shown in colored stick representation. (*B*) Ribbon representation of the most representative model of the C2A/PIP2 complex. Side chains of residues actively involved in the binding model are represented in sticks and colored in magenta and blue; the IP3 carbon ring of the PIP2 molecule is colored in green; and the DAG chain is colored in light gray.

Titration of the C2A domain with the PIP2 headgroup showed chemical shift deviations for restricted sets of HN cross-peaks expected for specific molecular interactions. The binding mode of IP3 to the C2A domain of rabphilin-3A involves two binding sites. The first one, with the highest affinity (i.e., $K_D = 55$ μM), involves the concave side of the domain including the basic patch located on β-strands 3 and 4 (Fig. 3A). The second binding site involves residues from the CBR (Fig. 3A). The affinity is about 10-fold weaker than for site 1 ($K_D > 500$ μM). Despite this low affinity, this interaction cannot be attributed to an affinity of the Ca^{2+}-loaded CBR for negatively charged phosphatidyl groups since no interaction was detectable in the case of the polar headgroup of PS. Therefore this second binding site is rather specific for IP3. Two IP3-binding sites have also been described for the C2 domain of PKCα (Corbalán-García et al. 2003).

The IP3-binding to the C2A domain has a Ca^{2+}-independent contribution (Fig. 4), but the binding is by far more effective when Ca^{2+} is present. On the other hand, the Ca^{2+} loading of the C2A domain is greatly enhanced by the presence of IP3. A similar behavior has been reported for the interaction of the C2B domain of synaptotagmin 1 with PIP2-containing liposomes (Bai et al. 2004; Li et al. 2006). This has been recently defined as the Target-Activated Messenger Affinity (TAMA) mechanism (Corbin et al. 2007). In this mechanism both the messenger and the target have to be simultaneously present to allow the protein to interact with them at physiological concentrations. This property described for the C2 domain of PKCα is responsible for the proper targeting of the entire protein to PIP2-enriched subdomains upon Ca^{2+} signaling (Sanchez-Bautista et al. 2006; Corbin et al. 2007). Based on the TAMA mechanism and by analogy to the PKCα–PIP2 interaction, the C2A domain may be involved in targeting rabphilin-3A to PIP2-enriched membrane subdomains. Noteworthy, a similar mechanism has been suggested for the PIP2-mediated interaction of the C2B domain of synaptotagmin 1 with t-SNAREs at physiological Ca^{2+} concentrations (Tucker et al. 2003).

C2A domain-PIP2 docking model

Until now, no NMR or crystallographic structure of a C2 domain in the complex with the PIP2 headgroup has been obtained. Furthermore, NMR structural studies with conventional methods, such as the measurement of RDCs or intermolecular NOEs, are hindered by the low affinity between C2 domains and IP3. In addition, due to the low proton density of the IP3 molecule (only five protons are located in the sugar ring), the use of specific NMR methods for the study of low affinity complexes, such as STD or Tr-NOESY experiments, is compromised. In these circumstances, chemical shift mapping is the only direct structural information available. It does not allow distinction between active (direct ligand interaction) and passive (no direct ligand interaction) residues. Thus, using a specific docking protocol might help to identify residues actively involved in the binding process even if it does not completely solve the inherent ambiguity of chemical shift mapping data. HADDOCK is a powerful docking approach exploiting ambiguous experimental data to drive docking calculations (Dominguez et al. 2003). Since chemical shift mapping was performed on the rabphilin-3A C2A domain upon IP3-binding, it was straightforward to use these data to generate a model of the C2A domain in complex with PIP2. This model provides a rather well defined relative protein–ligand positioning and orientation. In the C2A/PIP2 complex (Fig. 7A,B) PIP2 points perpendicularly toward the concave surface of the β-sheet, similar to its interaction with the C2 domain of PKCα (Guerrero-Valero et al. 2007). The docking model (Fig. 7B) suggests that the basic residues located on β-strands 3 and 4 contribute directly to the ligand binding. Analogously, these basic residues are conserved in the PKCα C2 domain and are essential for the interaction of this C2 domain with PIP2 (Rodríguez-Alfaro et al. 2004; Evans et al. 2006).

C2B domain-PIP2 binding

Although being the primary target of the C2B domain (Chung et al. 1998), a specific recognition of the phosphatidylserine headgroup by this domain could not be demonstrated in solution. C2B domain binding to PS is Ca^{2+} dependent and requires the membrane interface (Montaville et al. 2007). These observations are in line with an electrostatic switch function of Ca^{2+} between the CBRs of C2 domains and the negatively charged membrane surface rather than a specific phospholipid recognition (Lemmon 2008). On the other hand, IP3 binds to the basic concave side of the C2B domain similar to the interaction modes observed for the C2 domain of PKCα (Corbalán-García et al. 2003), the C2A domain of rabphilin-3A (as shown here), and the C2B domain of synaptotagmin (Schiavo et al. 1996). However, PIP2 headgroup binding only slightly involves the conserved polybasic motif in β-strand 4 as shown by the IP3 titration (Fig. 5A). In light of a recent study describing the role of the polybasic motif on β-strand 4 of the C2B domain for SNAP25 binding (Tsuboi et al. 2007), it is remarkable that only K595 and K593 from the polybasic stretch are involved in the IP3 interaction (Fig. 5A). The other basic residues in this region (K590, K591, H594, K599, K600, and K601) would be still available for SNAP25 interaction. Thus, simultaneous binding of PIP2 and SNAP25 to the C2B domain would be possible. Noteworthy, it has been shown that t-SNARE lateral diffusion in reconstituted phospholipid bilayers is lowered in the presence of PIP2

(Wagner and Tamm 2001), and it has been recently shown that PIP2 and SNAP25 co-localize within specific subdomains of the plasma membrane in PC12 cells (Aikawa et al. 2006).

The C2B domain of rabphilin-3A exhibits completely different IP3-binding properties compared to the C2A domain. It binds IP3 in a Ca^{2+}-independent fashion and with a relatively low affinity in solution ($K_D = 0.5$ mM) (Fig. 5C). This has been observed for other C2 domains. For example, the C2B domain of synaptotagmin 9 binds PIP2 also in a Ca^{2+}-independent way (Tucker et al. 2003). The Ca^{2+}-independent mode of the PIP2 headgroup recognition by the C2B domain of rabphilin-3A in solution is not in contradiction with its Ca^{2+}-dependent binding to PIP2-containing liposomes (Chung et al. 1998). In that study the authors had shown a greatly increased ability of the C2B domain to interact with liposomes containing 19% PS and 0.36% PIP2 compared to liposomes where PIP2 was not incorporated. The strong increase in interaction could not be exclusively explained by the increase of the negative surface charge following incorporation of PIP2 into the liposomes. Instead, a specific interaction of the C2B domain with PIP2 was postulated. Moreover, in the same study the binding of the C2B domain to PI(4,5)P2-containing liposomes was shown to be far more efficient than the binding to PI(3,4)P2-containing liposomes (Chung et al. 1998). Consequently, the Ca^{2+}-independent character of this specific interaction, as well as its low affinity in solution, suggest that this interaction should occur after the C2B domain has bound to PS in a Ca^{2+}-dependent manner at the membrane interface. Thus, PIP2 appears to be an effector of the C2B domain rather than a target, as suggested above for the C2A domain.

By the present work, we characterized the binding properties of the rabphilin-3A C2 domains for the PIP2 headgroup in terms of affinity, Ca^{2+} dependency, and binding sites. Moreover, we were able to propose a valuable model of the C2A domain in complex with PIP2, supporting the experimental data. These results, taken together, demonstrate a strong asymmetry of the two C2 domains of rabphilin-3A with respect to the PIP2 headgroup interaction. In the context of vesicle trafficking, PIP2 should clearly be a target of the C2A domain while this phospholipid is probably an effector of the C2B domain. Future in vivo investigations of both C2 domain–PIP2 interactions should provide a better insight into the functional implications of rabphilin-3A in vesicle trafficking.

Materials and Methods

Sample preparation

The C2A (fragment 371–510) and C2B (fragment 519–684) domains of rat rabphilin-3A were prepared as described previously (Biadene et al. 2006; Montaville et al. 2007). The ^{15}N labeled domains were obtained by expressing the protein in minimal medium containing ^{15}N-labeled ammonium chloride as the sole nitrogen source. All samples were concentrated up to 0.5 mM in 50 mM HEPES, pH 7.0, 150 mM NaCl, and 1 mM DTT supplemented with 10% D_2O.

NMR measurements

NMR experiments were carried out with a DRX 700 MHz Bruker spectrometer, equipped with a TXI 3 axes gradient probe at 298K. All spectra were processed using NMRPipe/NMRDraw (Delaglio et al. 1995) and analyzed with Sparky (http://www.cgl.ucsf.edu/home/sparky/). D-myo-Inositol-1,4,5-trisphosphate (IP3) from Calbiochem was used to perform ^{15}N-^{1}H HSQC based titrations. Glycerophosphoserine was chemically synthesized according to patent WO/05024, and 1,2-dioctanoyl-PIP2 (DOPIP2) was purchased from Avanti Polar Lipids. The assignments of HN cross-peaks were taken from the BMRB entry 6787 for the C2A domain (Montaville et al. 2006) and the BMRB entry 4360 for the C2B domain (Ubach et al. 1999).

Fitting procedure

To evaluate titration experiments of the labeled C2 domains with Ca^{2+} and IP3 the chemical shift deviations of significantly affected residues were plotted against the ligand concentration. Simultaneous fit was performed using Igor Pro (Wavemetrics, Inc.) with the following equations. Single binding-site model (Auguin et al. 2004):

$$\Delta\delta\text{ppm} = B_{max} \frac{[Pt] + [Lt] + K_D - \sqrt{([Pt] + [Lt] + K_D)^2 - 4[Pt][Lt]}}{2[Pt]} \tag{1},$$

where $[Pt]$, $[Lt]$, K_D, and B_{max} are the total protein concentration, ligand concentration, dissociation constant, and chemical shift deviation at saturation, respectively.

For fitting HN chemical shift perturbations upon IP3 titrations of residues belonging to a second binding site with a lower affinity than the first binding site, the total ligand concentration had to be adjusted to take into account the binding of the ligand in the high affinity-binding site:

$$\Delta\delta\text{ppm} = B_{max} \left(\frac{[Pt] + [Lt] - A + K_{D2} - \sqrt{([Pt] + [Lt] - A + K_{D2})^2 - 4[Pt]([Lt] - A)}}{2[Pt]} \right) \tag{2},$$

where

$$A = \frac{[Pt] + [Lt] + K_{D1} - \sqrt{([Pt] + [Lt] + K_{D1})^2 - 4[Pt][Lt]}}{2},$$

and $[Pt]$, $[Lt]$, K_{D1}, K_{D2}, and B_{max} are the total protein concentration, ligand concentration, dissociation constant of the

first site (higher affinity), dissociation constant of the second site (lower affinity), and the chemical shift deviation at saturation, respectively. *A* represents the ligand concentration bound to the higher affinity-binding site according to Equation 1. Consequently, $[Lt]$-*A* is the total ligand concentration experienced by the binding site of lower affinity.

For the cooperative binding model, the total ligand concentration was used in the Hill equation to calculate the free ligand concentration:

$$\Delta\delta\text{ppm} = B_{\max} \frac{\left([Lt] - \left(\frac{[Pt]+[Lt]+K_{Dapp} - \sqrt{\left([Pt]+[Lt]+K_{Dapp}\right)^2 - 4[Pt][Lt]}}{2} \right) \right)^n}{K_{Dapp}{}^n + \left([Lt] - \left(\frac{[Pt]+[Lt]+K_{Dapp} - \sqrt{\left([Pt]+[Lt]+K_{Dapp}\right)^2 - 4[Pt][Lt]}}{2} \right) \right)^n}$$

(3)

where $[Pt]$, $[Lt]$, K_{Dapp}, n, and $B_{\max}$ are the total protein concentration, ligand concentration, global dissociation constant, the Hill coefficient, and chemical shift deviation at saturation, respectively.

Docking model for C2A domain–PIP2 complex

The model of the C2A/PIP2 complex was calculated using the docking program HADDOCK (Dominguez et al. 2003) in combination with CNS (Brunger et al. 1998). Coordinates for the rabphilin-3A C2A domain were taken from the Protein Data Bank (entry 2CHD) (Biadene et al. 2006). Coordinates for IP3 ligand were extracted from the crystal structure of the inositol 1,4,5-trisphosphate receptor binding core in complex with IP3 (entry 1N4K) (Bosanac et al. 2002), then the PIP2 ligand was designed by adding a 1,2-diacetoyl-sn-glycerol group (diacylglycerol, DAG) to IP3 (in position 1) using the builder module in InsightII, followed by a short minimization protocol using Discover (Hill and Sauer 1994; Hwang et al. 1994; Maple et al. 1994). The topology and parameter files were generated using the PRODGR2 server (Schuttelkopf and van Aalten 2004).

The docking procedure was driven using only ambiguous intermolecular restraints, which were defined based on the chemical shift perturbations ($\Delta\delta$) observed for C2A amide groups upon ligand binding. Only solvent-accessible residues undergoing significant chemical shift perturbation ($\Delta\delta$ larger than 0.1 ppm) were defined as active residues. Since titration experiments were performed with IP3, the PIP2 molecule was treated as two residues (the DAG group and the IP3 core). Only the IP3 core was defined as an active residue. IP3 was kept rigid in order to maintain the boat conformation of the inositol ring. The DAG group was set as fully flexible. The docking calculations were performed with HADDOCK 2.0, using Optimized Parameters for Liquid Simulation and bonded parameters from parallhdg5.3.pro force field. More details about the docking protocol including a list of active residues and a full description of the docking consecutive stages are summarized in Supplemental Table 1. The 50 structures obtained after water refinement were analyzed and ranked according to their HADDOCK score (Supplemental Table 2). The three best models were selected as the final representative ensemble of the complex structure.

Electronic supplemental material

Supplemental Table 1 shows the docking protocol and input parameters. Supplemental Table 2 presents the structural statistics for the final ensembles of 50 structures for the protein/ligand models. In Supplemental Figure 1 the hydrogen bond network involving E678 and C2B core domain residues is shown in a ribbon presentation of the crystal structure of the C2B domain.

Acknowledgments

References

Aikawa, Y., Xia, X., and Martin, T.F. 2006. SNAP25, but not syntaxin 1A, recycles via an ARF6-regulated pathway in neuroendocrine cells. *Mol. Biol. Cell* **17:** 711–722.

Auguin, D., Barthe, P., Royer, C., Stern, M.H., Noguchi, M., Arold, S.T., and Roumestand, C. 2004. Structural basis for the co-activation of protein kinase B by T-cell leukemia-1 (TCL1) family proto-oncoproteins. *J. Biol. Chem.* **279:** 35890–35902.

Bai, J., Tucker, W.C., and Chapman, E.R. 2004. PIP2 increases the speed of response of synaptotagmin and steers its membrane-penetration activity toward the plasma membrane. *Nat. Struct. Mol. Biol.* **11:** 36–44.

Baldini, G., Martelli, A.M., Tabellini, G., Horn, C., Machaca, K., Narducci, P., and Baldini, G. 2005. Rabphilin localizes with the cell actin cytoskeleton and stimulates association of granules with F-actin cross-linked by α-actinin. *J. Biol. Chem.* **280:** 34974–34984.

Biadene, M., Montaville, P., Sheldrick, G.M., and Becker, S. 2006. Structure of the C2A domain of rabphilin-3A. *Acta Crystallogr. D Biol. Crystallogr.* **62:** 793–799.

Bosanac, I., Alattia, J.R., Mal, T.K., Chan, J., Talarico, S., Tong, F.K., Tong, K.I., Yoshikawa, F., Furuichi, T., Iwai, M., et al. 2002. Structure of the inositol 1,4,5-trisphosphate receptor binding core in complex with its ligand. *Nature* **420:** 696–700.

Brunger, A.T., Adams, P.D., Clore, G.M., DeLano, W.L., Gros, P., Grosse-Kunstleve, R.W., Jiang, J.S., Kuszewski, J., Nilges, M., Pannu, N.S., et al. 1998. Crystallography & NMR system: A new software suite for macromolecular structure determination. *Acta Crystallogr. D Biol. Crystallogr.* **54:** 905–921.

Cho, W. and Stahelin, R.V. 2006. Membrane binding and subcellular targeting of C2 domains. *Biochim. Biophys. Acta* **1761:** 838–849.

Chung, S.H., Song, W.J., Kim, K., Bednarski, J.J., Chen, J., Prestwich, G.D., and Holz, R.W. 1998. The C2 domains of Rabphilin3A specifically bind phosphatidylinositol 4,5-bisphosphate containing vesicles in a Ca²⁺-dependent manner. In vitro characteristics and possible significance. *J. Biol. Chem.* **273:** 10240–10248.

Corbalán-García, S., García-García, J., Rodríguez-Alfaro, J.A., and Gómez-Fernández, J.C. 2003. A new phosphatidylinositol 4,5-bisphosphate-binding site located in the C2 domain of protein kinase Cα. *J. Biol. Chem.* **278:** 4972–4980.

Corbin, J.A., Evans, J.H., Landgraf, K.E., and Falke, J.J. 2007. Mechanism of specific membrane targeting by C2 domains: Localized pools of target lipids enhance Ca²⁺ affinity. *Biochemistry* **46:** 4322–4336.

Cremona, O. and De Camilli, P. 2001. Phosphoinositides in membrane traffic at the synapse. *J. Cell Sci.* **114:** 1041–1052.

Deak, F., Shin, O.H., Tang, J., Hanson, P., Ubach, J., Jahn, R., Rizo, J., Kavalali, E.T., and Sudhof, T.C. 2006. Rabphilin regulates SNARE-dependent re-priming of synaptic vesicles for fusion. *EMBO J.* **25:** 2856–2866.

Delaglio, F., Grzesiek, S., Vuister, G.W., Zhu, G., Pfeifer, J., and Bax, A. 1995. NMRPipe: A multidimensional spectral processing system based on UNIX pipes. *J. Biomol. NMR* **6:** 277–293.

Dominguez, C., Boelens, R., and Bonvin, A.M. 2003. HADDOCK: A protein–protein docking approach based on biochemical or biophysical information. *J. Am. Chem. Soc.* **125:** 1731–1737.

Evans, J.H., Murray, D., Leslie, C.C., and Falke, J.J. 2006. Specific trans-location of protein kinase Cα to the plasma membrane requires both Ca^{2+} and PIP2 recognition by its C2 domain. *Mol. Biol. Cell* **17:** 56–66.

Golub, T. and Caroni, P. 2005. PI(4,5)P2-dependent microdomain assemblies capture microtubules to promote and control leading edge motility. *J. Cell Biol.* **169:** 151–165.

Grishanin, R.N., Kowalchyk, J.A., Klenchin, V.A., Ann, K., Earles, C.A., Chapman, E.R., Gerona, R.R., and Martin, T.F. 2004. CAPS acts at a prefusion step in dense-core vesicle exocytosis as a PIP2 binding protein. *Neuron* **43:** 551–562.

Guerrero-Valero, M., Marín-Vicente, C., Gómez-Fernández, J.C., and Corbalán-García, S. 2007. The C2 domains of classical PKCs are specific PtdIns(4,5)P(2)-sensing domains with different affinities for membrane binding. *J. Mol. Biol.* **371:** 608–621.

Haucke, V. 2005. Phosphoinositide regulation of clathrin-mediated endocytosis. *Biochem. Soc. Trans.* **33:** 1285–1289.

Hill, J.R. and Sauer, J. 1994. Molecular mechanics potential for silica and zeolite catalysts based on ab initio calculations. 1. Dense and microporous silica. *J. Phys. Chem.* **98:** 1238–1244.

Hwang, M.J., Stockfisch, T.P., and Hagler, A.T. 1994. Derivation of class II force fields. 2. Derivation and characterization of a class II force field, CFF93, for the alkyl functional group and alkane molecules. *J. Am. Chem. Soc.* **116:** 2515–2525.

Lemmon, M.A. 2008. Membrane recognition by phospholipid-binding domains. *Nat. Rev. Mol. Cell Biol.* **9:** 99–111.

Li, L., Shin, O.H., Rhee, J.S., Arac, D., Rah, J.C., Rizo, J., Sudhof, T., and Rosenmund, C. 2006. Phosphatidylinositol phosphates as co-activators of Ca^{2+} binding to C2 domains of synaptotagmin 1. *J. Biol. Chem.* **281:** 15845–15852.

Maple, J.R., Hwang, M.-J., Stockfisch, T.P., Dinur, U., Waldman, M., Ewig, C.S., and Hagler, A.T. 1994. Derivation of class II force fields. I. Methodology and quantum force field for the alkyl functional group and alkane molecules. *J. Comput. Chem.* **15:** 162–182.

Marín-Vicente, C., Gómez-Fernández, J.C., and Corbalán-García, S. 2005. The ATP-dependent membrane localization of protein kinase Cα is regulated by Ca^{2+} influx and phosphatidylinositol 4,5-bisphosphate in differentiated PC12 cells. *Mol. Biol. Cell* **16:** 2848–2861.

Miyazaki, M., Shirataki, H., Kohno, H., Kaibuchi, K., Tsugita, A., and Takai, Y. 1994. Identification as β-adducin of a protein interacting with rabphilin-3A in the presence of Ca^{2+} and phosphatidylserine. *Biochem. Biophys. Res. Commun.* **205:** 460–466.

Montaville, P., Kim, H.Y., Vijayan, V., Becker, S., and Zweckstetter, M. 2006. ^{1}H, ^{15}N, and ^{13}C resonance assignment of the C2A domain of rabphilin 3A. *J. Biomol. NMR* (Suppl 1):**36:** 20.

Montaville, P., Schlicker, C., Leonov, A., Zweckstetter, M., Sheldrick, G.M., and Becker, S. 2007. The C2A-C2B linker defines the high affinity Ca^{2+} binding mode of rabphilin-3A. *J. Biol. Chem.* **282:** 5015–5025.

Ohya, T., Sasaki, T., Kato, M., and Takai, Y. 1998. Involvement of Rabphilin3 in endocytosis through interaction with Rabaptin5. *J. Biol. Chem.* **273:** 613–617.

Osborne, S.L., Wen, P.J., and Meunier, F.A. 2006. Phosphoinositide regulation of neuroexocytosis: Adding to the complexity. *J. Neurochem.* **98:** 336–342.

Rodríguez-Alfaro, J.A., Gómez-Fernández, J.C., and Corbalán-García, S. 2004. Role of the lysine-rich cluster of the C2 domain in the phosphatidylserine-dependent activation of PKCα. *J. Mol. Biol.* **335:** 1117–1129.

Sanchez-Bautista, S., Marín-Vicente, C., Gómez-Fernández, J.C., and Corbalán-García, S. 2006. The C2 domain of PKCα is a Ca^{2+}-dependent PtdIns(4,5)P2 sensing domain: A new insight into an old pathway. *J. Mol. Biol.* **362:** 901–914.

Schiavo, G., Gu, Q.M., Prestwich, G.D., Sollner, T.H., and Rothman, J.E. 1996. Calcium-dependent switching of the specificity of phosphoinositide binding to synaptotagmin. *Proc. Natl. Acad. Sci.* **93:** 13327–13332.

Schuttelkopf, A.W. and van Aalten, D.M. 2004. PRODRG: A tool for high-throughput crystallography of protein-ligand complexes. *Acta Crystallogr. D Biol. Crystallogr.* **60:** 1355–1363.

Tsuboi, T. and Fukuda, M. 2005. The C2B domain of rabphilin directly interacts with SNAP-25 and regulates the docking step of dense core vesicle exocytosis in PC12 cells. *J. Biol. Chem.* **280:** 39253–39259.

Tsuboi, T., Kanno, E., and Fukuda, M. 2007. The polybasic sequence in the C2B domain of rabphilin is required for the vesicle-docking step in PC12 cells. *J. Neurochem.* **100:** 770–779.

Tucker, W.C., Edwardson, J.M., Bai, J., Kim, H.J., Martin, T.F., and Chapman, E.R. 2003. Identification of synaptotagmin effectors via acute inhibition of secretion from cracked PC12 cells. *J. Cell Biol.* **162:** 199–209.

Ubach, J., Garcia, J., Nittler, M.P., Sudhof, T.C., and Rizo, J. 1999. Structure of the Janus-faced C2B domain of rabphilin. *Nat. Cell Biol.* **1:** 106–112.

Wagner, M.L. and Tamm, L.K. 2001. Reconstituted syntaxin1a/SNAP25 interacts with negatively charged lipids as measured by lateral diffusion in planar supported bilayers. *Biophys. J.* **81:** 266–275.

Willshaw, A., Grant, K., Yan, J., Rockliffe, N., Ambavarapu, S., Burdyga, G., Varro, A., Fukuoka, S., and Gawler, D. 2004. Identification of a novel protein complex containing annexin A4, rabphilin and synaptotagmin. *FEBS Lett.* **559:** 13–21.

Yamaguchi, T., Shirataki, H., Kishida, S., Miyazaki, M., Nishikawa, J., Wada, K., Numata, S., Kaibuchi, K., and Takai, Y. 1993. Two functionally different domains of Rabphilin-3A, *Rab*3A p25/*smg* p25A-binding and phospholipid- and Ca^{2+}-binding domains. *J. Biol. Chem.* **268:** 27164–27170.

Zhang, Y., Luan, Z., Liu, A., and Hu, G. 2001. The scaffolding protein CASK mediates the interaction between rabphilin3a and β-neurexins. *FEBS Lett.* **497:** 99–102.